11

Long Period Fibre Gratings

Alejandro Martinez-Rios, David Monzon-Hernandez,
Ismael Torres-Gomez and Guillermo Salceda-Delgado
Centro de Investigaciones en Optica, Leon, Guanajuato
Mexico

1. Introduction

In essence, a long period fibre grating (LPFG) is an all-fibre device with wavelength dependent loss. As a band rejection filter, all light in a spectral slice is discarded without affecting the amplitude and phase of neighbouring wavelengths, with the additional advantage of low insertion losses and minimum backreflection (Daxhelet, 2003). LPFGs have been used as band rejection filters, sensors, wavelength selective elements in fibre lasers and amplifiers (Su &Wang, 1999), beam shaping (Mohamed & Gu,2009), etc. In addition, in-series LPFG pairs can be used to form all-fibre Mach-Zender interferometers that are useful as wavelength selective filters for WDM applications; while parallel LPFGs act as wavelength selective couplers or wavelength multiplexers (Chan & Yasumoto, 2007; Shu et. al.,2002). In a common LPFG, the core mode couples to co-propagating cladding modes supported by the cladding-external medium waveguide structure. The specific cladding through which the core mode is coupled is determined by the following resonance condition:

$$\frac{2\pi}{\Lambda} = \frac{2\pi}{\lambda}\left(n_{eco} - n_{ecla}^{i}\right)$$

(1)

where n_{eco} is the effective index of the fundamental core mode, n_{ecla}^{i} is the effective index of the ith cladding mode, λ is the resonance wavelength, i.e. the wavelength where the notch band is formed, and Λ is the period of the grating. As can be clearly seen from this relation the resonance wavelength is determined by the effective refractive indices of the core and cladding modes, so that any geometrical, photo-induced, thermal-induced, or mechanically-induced change (periodic) will modify the position of the resonance wavelength. This property is what makes LPFGs so useful for applications in fields as diverse as optical sensing, biological and chemical sensing, as wavelength dependent loss elements in telecommunication systems and laser and many more. In this chapter we will make a review of the relevant aspects of LPFGs. In section 2.2 we will review the fabrication methods used to write LPFGs in optical fibres; in section 3 we will review the theory behind the operation of LPFGs; in section 4 we will talk about the applications of LPFGs; and, in section 5 we give the conclusions of the present chapter.

2. Fabrication methods of long-period fibre gratings

The inscription of long-period gratings on optical fibre basically consists in the generation of a periodical perturbation of the refractive index in the core, the cladding, or both along the

optical fibre (Vengsarkar, 1996). The refractive index perturbation requires a length of 3-5 cm, an amplitude in the range of 10^{-4} to 10^{-5} similar to Bragg gratings. In contrast, the perturbation period in LPFGs is usually larger than 100 μm, which is two orders larger than Bragg gratings. In this way, different physical properties of the optical fibre glass or the variation of the optical fibre structure can be used to produce this periodical refractive index perturbation in the fibre, such as; the UV photosensitivity, the residual thermal stress, the photoelasticity and the geometrical modulation of the cladding structure (Hill et. al., 1990; Dianov et. al. 1997; Rao et. al. 2004; Hwang et. al., 1999). In the first case, an ultraviolet light source is used to write the core index modulation in Ge-doped fibres by the photosensitive mechanism, on the other hand, a heating source such as a CO_2 laser (Hwang et. al., 1999), or an electric arc system (Bjarklev, 1986), are employed to produce simultaneously the index modulation in the core and the cladding via the residual thermal stress. In a similar way, a mechanical pressure system temporally produces the index modulation in the core and the cladding by the photoelasticity effect (Savin et. al. 2000). Meanwhile, the geometrical modulation of the cladding structure can be done by chemical etching (Vaziri & Chin-Lin, 1997) and other methods. Except the UV photosensitive mechanism, the others one can be used in any type of optical fibre.

In the last 15 years, alternative writing methods of long-period fibre gratings have been proven after the demonstration of UV radiation method. Some of the most used methods include; the heating, the mechanical stress and chemical etching between others (Fujimaki et. al.,2000; Jeong et. al., 2000). The inscription method and the optical fibre type impact in the physical properties and optical spectral transmission characteristics of the rejection bands of the LPFGs. Each inscription method produces a particular transversal and longitudinal refractive index profile. The transversal index profile determines the mode coupling between the core fundamental mode and the cladding discrete high order modes involved (Anemogiannis et. al., 2003). Meanwhile, the longitudinal index profile determines the location and shape of the rejection loss bands (DeLisa et. al., 2000). The combination of the total index profile and the fibre type define the optical properties of the rejection bands such as; position of the central resonant wavelength, bandwidth, isolation depth, insertion loss, induced birefringence, and polarization dependent loss. In the same way, this combination directly influence in the rejection bands sensitivity to physical variables such as; temperature, tension, torsion, bending, and external refractive index.

The post-processing of LPFGs is actually used to adjust or stabilize the spectral transmission, as well to improve the sensitivity of the rejection bands in the LPFGs. The sensitivity improve or sensitization of the rejection band to a particular external parameter include, the deposition of some materials over the LPFG (Gu et. al., 2006) and the etching process to reduce the cladding diameter to expose the high cladding modes to the external medium (Chiang et. al., 2001). On other hand, the annealing process is used to tune and stabilize the attenuation bands of the LPFGs (Ng & Chiang, 2002).

2.1 UV long-period fibre gratings

There are two common techniques to inscribe a LPFG in Ge-doped optical fibres by using the UV radiation method: the amplitude mask and the point to point technique (Othonos & Kalli, 1999; Vengsarkar, 1996). The key parameters in the UV inscription method of the LPFG over the Ge-doped fibres are: the UV selected wavelength (193-360 nm), the density

power of the laser, and the exposition time (Othonos & Kalli, 1999). In the first technique, the optical fibre is scanned by the UV beam through an amplitude mask (AM) as is illustrated by Fig. 1(a). The AM contains an array of transparent windows that forms an illuminated-shadow periodical pattern with a period Λ over the fibre. In case of low UV sensitivity optical fibres, the hydrogenation or the flame brushing process can be used to improve the UV sensitivity in low Ge-doped fibres (Lemaire et. al., 1993; Bilodeau et. al., 1993). Actually, B-Ge codoped optical fibres have been developed to achieve high UV sensitive optical fibre (Williams et. al., 1993). In the point to point technique, the UV beam illuminates a section the optical fibre by a thin slit aperture (S). In this setup, the beam spot is fixed and the optical fibre moves in the z exes with a period Λ. Both techniques are relative simple to implement; however, the first one is more attractive to mass production, although the point to point technique is more flexible and cheaper than the amplitude mask technique. The main limitation of this technique is that only works in UV photosensitivity fibre.
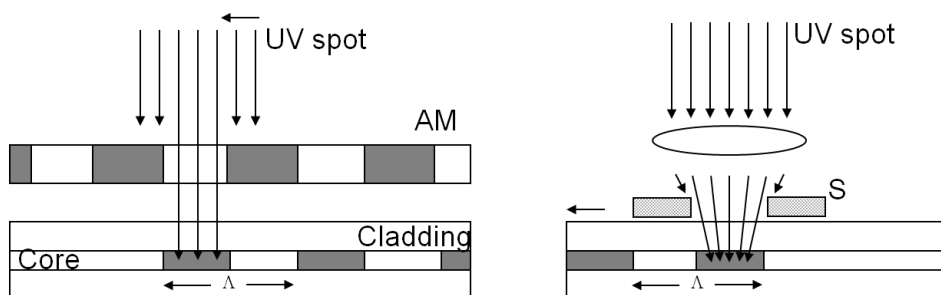

Fig. 1. LPFG inscription by the UV techniques: a) phase amplitude mask, b) point to point.

The expected z index profile with UV techniques is Gaussian and azimuthally uniform in the transversal plane. In this case, this profile supports the mode coupling between the fundamental mode LP_{01} in the core and the discrete LP_{0m} in the cladding. The main spectrum transmission characteristics of the rejection bands of UV LPFGs are: wide range wavelength location from visible to infrared, the lowest loss insertion loss < 0.2 dB, the isolation depth is larger than 25 dB and the lowest induced birefringence group. The disadvantages of UV induced LPFGs are temperature limited operation range <250º C and high cost fabrication. The table 1 displays some properties and the sensitivities to some physical parameters. Because the UV LPFG couples modes with azimuthal symmetry the rejection bands are not sensible to twist or bending direction.

2.2 Residual thermal stress long period fibre gratings

The heating and fast cool down of the glass alter the viscosity, it in turns, slightly modified the refractive index. In this case, the heating process and follow by a fast cool, of the glass can be use to froze a periodical index modulation across the optical fibre structure (core and cladding). There are two used methods to generate the periodical index modulation by CO_2 radiation (heating absorption) and electrical arc. Both methods can be use in any kind of fibre. These methods induce a no uniform refractive index profile in the transversal plane, allowing the coupling to symmetric and asymmetric cladding modes. In the CO_2 radiation

method, the optical fibre under tension is radiated though a germanium lenses with a infrared signal at 10 µm point to point. At this wavelength, the silica is not transparent and absorbs the energy from the CO_2 laser, so that the fibre is heated and cooled at room temperature. The required power in optical fibres is 10 W in continuous wave CO_2 lasers. On the other hand, in the electric arc discharge method, the optical fibre is heated by an electric arc generated usually by a fusion splicing machine. For standard optical fibres, the parameters of electric arc discharge are: 200 ms, current 50 mA at tension of few grams. According with the price arc discharge method is cheaper than CO_2 laser.

The spectral characteristics of thermal induced LPFGs are high stability in wide range of temperature, low loss insertion loss. The disadvantages of thermal induced LPFGs are: the loss bands shift and the depth decrease of the bands with the time.
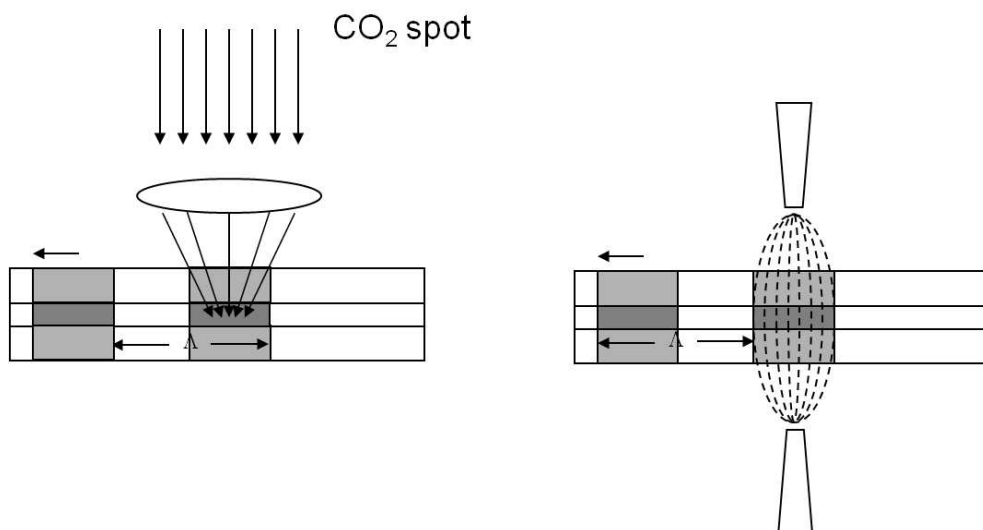

Fig. 2. LPFG inscription by thermal stress techniques; a) CO_2 irradiation, b) electric arc discharge

2.3 Mechanical stress induced long period fibre gratings

The optical refractive index of glass can be modulated when the glass is exposed to stress. This change in optical refractive index is due to the photo-elastic response of glass. In this case, the photo-elasticity can be used to induce a temporal periodical modulation of the refractive index in the core and the cladding to generate long-period fibre gratings. According to this, microbending and periodical pressure points in the fibre can be used to induce long-period fibre gratings. Different techniques have been reported to generate microbending such as: metallic grooved plates, strings, flexure acoustic waves. In the case of periodical pressure points; metallic grooved plates, coils springs and torsion. Figure 3 illustrates a typical example of periodical microbending and pressure points. Because, its flexibility and cost relation plates can be use for microbending or pressure is one of the most used techniques. This technique presents many variants in the corrugated design.
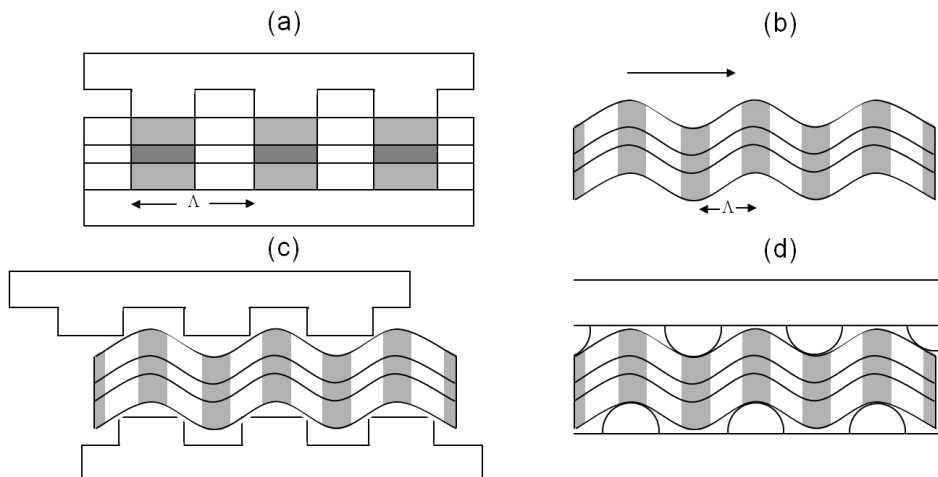
Fig. 3. Stress induced LPFGs, pressure points (a,b) microbending (c,d)

The photoelasticity of the glass allows the inscription of LPFGs practically in any kind of fibre, this include, standard telecommunication fibres, photonic crystal fibres, between others. The amplitude of the refractive index periodical perturbation is the order of 10^{-4} to 10^{-5}, so the pressure requite is less than 500 gr cm^{-1}, in the microbending case, the amplitude of the perturbation needed is in order of 200- 500 µm. The stress induced LPFGs present loss bands with attractive and flexible spectral transmission optical properties. The loss bands are erasable, simple control of the depth (0-20 dB), bandwidth control (10-50 nm) and a large tuning range >250 nm. The drawbacks are high sensitivity to ambient temperature, and insertion loss are in the order of 0.2- 0.3 dB.

2.4 Etching induced long-period fibre gratings

The effective index in the core can be modulated by the geometric modulation of the optical fibre diameter by etching chemical method. The etching induced LPFGs are also known as corrugated LPFGs. This method, consist in locate a photomask over the fibre, and then the optical fibre is immersed in a hydrofluoric acid solution, in this way alternated regions of the fibre are protected of the hydrofluoric solution meanwhile other regions are divested hydrofluoric attack on the silica glass. The diameter in the desvasted regions is controlled by the exposition time, as illustrated in the figure 4. This method is not as popular as UV, thermal or mechanical stress because, their low repeatability and the difficult control of corrugated structured of the fibre. Physically the corrugated LPFGs are fragile to tension or beding stress. The loss bands are high sensitivity to twist because the torsion stress focus in the core diameter.
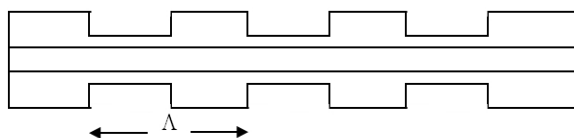

Fig. 4. Corrugated LPFG

Properties	UV	Residual thermal stress	Mechanical stress	Etching
Length [cm]	2 – 4	2 – 5	3 – 5	2 – 3
Isolation depth [dB]	10 – 30	10 – 25	10 – 20	10 – 15
$\Delta\lambda$ [nm]	> 10	> 10	> 15	> 10
Insertion loss [dB]	0.1 – 0.2	0.1 – 1	0.1 – 0.5	0.1 – 0.3
Modal birefringence	$2(10)^{-7}$	$1.7(10)^{-6}$	$7(10)^{-6}$	––
Λ [μm]	> 100	> 300	> 250	> 500
σ_T [nm /°C]	- (0.04– 0.347)	$\pm$(0.05 – 0.204)	0.180 – 200	––
σ_τ [nm /(rad/cm)]	15 –	$\pm$ (6.7 – 25)	6 – 12	-(70 – 100)
σ_σ [pm/$\mu\varepsilon$]	0.204 – 1.34	0.1 – 0.4	0.2 – 0.4	1.5 – 2
σ_b [nm/m]	2.5 – 14	-(1.6 – 12)	––	-(18 – 25)
$\sigma_{ext.\ index}$ [nm/10^{-3}]	-(0.003 – 0.019)	-(0.017 – 0.54)	0.22 – 0.5	––
Range of temperature operation [°C]	< 250	< 1100	< 60	< 1200

Mode order: m = 3rd,4th.   Ranges: [Λ=550-650 nm][σ_T:0-200°C], [σ_τ:0-5 rad/cm], [σ_σ:0-1000 $\mu\varepsilon$], [σ_b:0-5 m^{-1}], [$\sigma_{ext.\ index}$:1-1.3].

Table 1. Rejection bands properties reported in LPFG with different fabrication methods.

3. Theory of long period gratings

In this section we review the theoretical framework to describe long-period fibre gratings. We consider the most common case of a step-index fibre with three layers: the central core, the cladding, and the external medium. We follow the analysis given by Erdogan (Erdogan, 1997) for the calculation of the core and cladding effective refractive indices.

3.1 Characteristic equation for core and cladding modes

The most important parameter for the modelling of long period-fibre gratings are the effective indices of the core and cladding modes, which determine the coupling wavelength between co-propagating modes according to the following relation:

$$\lambda_{res} = (n_{efco} - n_{efcla})\Lambda \tag{2}$$

where λ_{res} is the resonance wavelength, n_{efco} is the effective index of the core mode, assumed to be single-mode, n_{efcla} is the effective index of a given cladding mode, and L is the period of the refractive index modulation. Here, for the calculation of the effective index, we consider that the core mode is not affected by the external medium that surrounds the cladding, so that the cladding can be considered as an infinitum medium as far as the core modes concerns. In this particular case, the characteristic equation from which the effective index of the core fundamental mode can be written as (Erdogan):

$$V\sqrt{1-b}\,\frac{J_1(V\sqrt{1-b})}{J_0(V\sqrt{1-b})} = V\sqrt{b}\,\frac{K_1(V\sqrt{b})}{K_0(V\sqrt{b})} \tag{3}$$

where J_m is the first class Bessel function of mth-order, K_m is the modified Bessel function of second class and m-order, $V(=2\pi a_{core}NA/\lambda)$ is the normalized frequency, b is the normalized propagation constant, a_{core} is the core diameter, NA is the core numerical aperture, and λ is the light wavelength. Figure 5 shows a plot of effective index as a function of wavelength for the fundamental core mode of a fibre with parameters corresponding to standar SMF-28 fibre. This plot was calculated using the Mathematica-like code shown in Table 2.
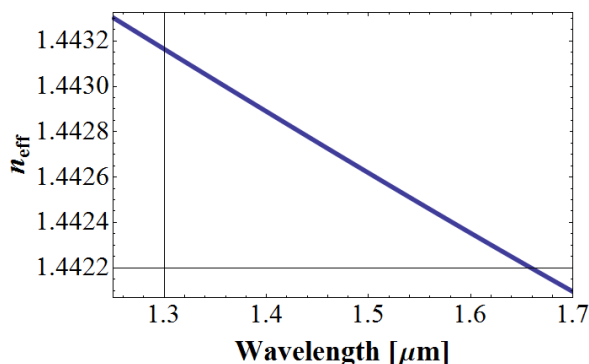

Fig. 5. Effective index of the fundamental core mode as a function of wavelength.

```
ClearAll("Global`*")
NA=0.14;  (*Numerical aperture*)
n1=1.4458;  (*Core refractive index*)
n2=Sqrt(n1^2-NA^2);   (*Cladding refractive index*)
a1=4.1;  (*Core radius*)
V[λ_,a_]=(2*Pi/λ)*a*NA; (*Normalized frequency*)
(*Argument of Bessel functions*)
c1[λ_,a_]=V[λ,a]*Sqrt[1-bw];
c2[λ_,a_]=V[λ,a]*Sqrt[bw];
(*Bessel functions*)
Jmn1=BesselJ[m-1,c1(λ,a)];Jmd1=BesselJ[m,c1(λ,a)]; Kmn1=BesselK[m-1,c2(λ,a)]; Kmd1=BesselK[m,c2(λ,a)];
(*Characteristic equation*)
fun1[a_,λ_,bw_,m_]=c1[λ,a]*(Jmn1/Jmd1)+c2[λ,a]*(Kmn1/Kmd1);
(*Plot the function to provide an approximated value for the normalized propagation constant*)
Plot[{fun1(a1,1.0,bw,0)},{bw,0,1}]
(*Calculation of the effective index of the core fundamental mode as a function of wavelength*)
ncore={{0,0}};
λ=1.7;  (*Initial wavelength*)

be1=0.45;  (*Initial value of the normalized propagation constant*)
(*For cycle to obtain the effective index at several wavelength*)
For[i=1,i<=450,i++,
r1=FindRoot[fun1(a1,\(Lambda),bw1,0)==0,{bw1,be1},WorkingPrecision->10];
nc=Sqrt[NA^2*r1[[1]][[2]]+n2^2];
ncore=Append[ncore,{λ,nc}];
λ=λ-0.001;];
nefco=Drop[ncore,1];  (*List of effective index versus wavelength *)
(*Plotting the effective index as a function of wavelength*)
ListPlot[{nefco},Frame->True,PlotRange->{{1.25,1.7},All},PlotStyle->Thickness(0.01),FrameLabel->{Style("Wavelength
(\(Mu)m)",Bold, 34),Style("Subscript(n, eff)",Bold, 34)},LabelStyle->Directive(Black,"Helvetica",32),Joined->True]
```

Table 2. Mathematica code for the calculation of the fundamental core mode effective index

In the case of the cladding modes the characteristic equation is given as (Erdogan, 1997):

$$\frac{1}{\sigma_2} \frac{u_2\left(J\cdot K + \dfrac{\sigma_1\sigma_2 u_{21}u_{32}}{n_2^2 a_1 a_2}\right)\cdot p_m(a_2) - K\cdot q_m(a_2) + J\cdot r_m(a_2) - \dfrac{1}{u_2}s_m(a_2)}{-u_2\cdot\left(\dfrac{u_{32}}{n_2^2 a_2}J - \dfrac{u_{21}}{n_1^2 a_1}K\right)\cdot p_m(a_2) + \dfrac{u_{32}}{n_1^2 a_2}q_m(a_2) + \dfrac{u_{21}}{n_1^2 a_1}r_m(a_2)}$$

$$= \sigma_1 \frac{u_2\left(\dfrac{u_{32}}{a_2}J - \dfrac{n_3^2\cdot u_{21}}{n_2^2\cdot a_1}\right)\cdot p_m(a_2) - \dfrac{u_{32}}{a_2}\cdot q_m(a_2) - \dfrac{u_{21}}{a_1}\cdot r_m(a_2)}{u_2\cdot\left(\dfrac{n_3^2}{n_2^2}J\cdot K + \dfrac{\sigma_1\sigma_2 u_{21}u_{32}}{n_1^2 a_1 a_2}\right)\cdot p_m(a_2) - \dfrac{n_3^2}{n_1^2}K\cdot q_m(a_2) + J\cdot r_m(a_2) - \dfrac{n_2^2}{n_1^2\cdot u_2}s_m(a_2)}$$

$$\tag{4}$$

where the parameters in (3) are defined by the following relations {Erdogan, 1997):

$$\sigma_{1`} = \frac{im}{\eta}\cdot n_{efcla} \quad ; \quad \sigma_{2`} = im\cdot\eta\cdot n_{efcla} \tag{5a}$$

$$u_{21} = \frac{1}{u_2^2} - \frac{1}{u_1^2} \quad ; \quad u_{32} = \frac{1}{w_3^2} - \frac{1}{u_2^2} \tag{5b}$$

$$u_1 = \frac{2\pi}{\lambda}\sqrt{n_1^2 - n_{efcla}^2} \quad ; \quad u_2 = \frac{2\pi}{\lambda}\sqrt{n_2^2 - n_{efcla}^2} \quad ; \quad w_3 = \frac{2\pi}{\lambda}\sqrt{n_{efcla}^2 - n_3^2} \tag{5c}$$

$$J = \frac{1}{2}\frac{J_{m-1}(u_1 a_1) + J_{m+1}(u_1 a_1)}{u_1 J_m(u_1 a_1)} \quad ; \quad K = -\frac{1}{2}\frac{K_{m-1}(w_3 a_2) - K_{m+1}(w_3 a_2)}{w_3 K_m(w_3 a_2)} \tag{5d}$$

$$p_m(r) = J_m(u_2 r)Y_m(u_2 a_1) - J_m(u_2 a_1)Y_m(u_2 r)$$
$$q_m(r) = \frac{1}{2}J_m(u_2 r)\big(Y_{m-1}(u_2 a_1) - Y_{m+1}(u_2 a_1)\big) - Y_m(u_2 r)\big(J_{m-1}(u_2 a_1) - J_{m+1}(u_2 a_1)\big)$$
$$r_m(r) = \frac{1}{2}Y_m(u_2 a_1)\big(Y_{m-1}(u_2 r) - Y_{m+1}(u_2 r)\big) \tag{5e}$$
$$s_m(r) = \frac{1}{4}\big(J_{m-1}(u_2 r) - J_{m+1}(u_2 r)\big)\big(Y_{m-1}(u_2 a_1) - Y_{m+1}(u_2 a_1)\big)$$
$$\quad -\big(J_{m-1}(u_2 a_1) - J_{m+1}(u_2 a_1)\big)\big(Y_{m-1}(u_2 r) - Y_{m+1}(u_2 r)\big)$$

where Y_m is a Bessel funtion of the the second kind, $\eta=(\mu_0/\varepsilon_0)^{1/2}$ is the vacuum impendance, and m is the azimuthal mode number. Figure 6 shows the calculated effective index difference between the fundamental core mode and the HE_{1m} (left graph) and HE_{2m} (right graph) cladding modes assuming a standard single-mode fibre, where we have used Eqs. (3) and (4) to find the effective refractive index of the core and cladding, respectively. Table 3 shows the Mathematica-like code used to calculate the effective index of the cladding modes.

```
(*Cladding modes*)
Z0=377;  (*Free space impedance*)
nco=n1;  (*Core refractive index*)
ncl=n2;  (*Cladding refractive index*)
acl=62.5;  (*Cladding radius*)
next=1;  (*External refractive index*)
NAcla=Sqrt(ncl^2-next^2);  (*Cladding numerical aperture*)
(*Parameters of the Erdogan Characteristic equation*)
σ1=I*m*nefcla/Z0;  σ2=I*m*nefcla*Z0;
u1=Sqrt((2*Pi/λ cla)^2*(nco^2-nefcla^2));  u2=Sqrt((2*Pi/λcla)^2*(ncl^2-nefcla^2));
w3=Sqrt((2*Pi/λcla)^2*(nefcla^2-next^2));
u21=(1/(u2^2))-(1/(u1^2));  u32=(1/(w3^2))+(1/(u2^2));
J=(1/2)*((BesselJ(m-1,u1*aco)+BesselJ(m+1,u1*aco))/(u1*BesselJ(m,u1*aco)));
Kp=(-1/2)*((BesselK(m-1,w3*acl)-BesselK(m+1,w3*acl))/(w3*BesselK(m,w3*acl)));
p(m_,r_)=BesselJ(m,u2*r)*BesselY(m,u2*aco)-BesselJ(m,u2*aco)*BesselY(m,u2*r);
q(m_,r_)=(1/2)*(BesselJ(m,u2*r)*(BesselY(m-1,u2*aco)-BesselY(m+1,u2*aco))
       -BesselJ(m,u2*r)*(BesselY(m-1,u2*aco)-BesselY(m+1,u2*aco)));
r(m_,r_)=(1/2)*(BesselY(m,u2*aco)*(BesselY(m-1,u2*r)-BesselY(m+1,u2*r)));
s(m_,r_)=(1/4)*((BesselJ(m-1,u2*r)-BesselJ(m+1,u2*r))*(BesselY(m-1,u2*aco)-
       BesselY(m+1,u2*aco))-(BesselJ(m-1,u2*aco)-BesselJ(m+1,u2*aco))*(BesselY(m-1,u2*r)-BesselY(m+1,u2*r)));
num1(m_)=(1/σ2)*((J*Kp+((σ1*\(Sigma)2*u21*u32)/(aco*acl*ncl^2)))*u2*p(m,acl)-Kp*q(m,acl)+J*r(m,acl)-
s(m,acl)/u2);
den1(m_)=-((u32/(acl*ncl^2))*J-
(u21/(aco*nco^2))*Kp)*u2*p(m,acl)+(u32*q(m,acl)/(acl*nco^2))+(u21*r(m,acl)/(aco*nco^2));
num2(m_)=σ 1*(((u32/acl)*J-u21*next^2/(aco*ncl^2))*Kp)*u2*p(m,acl)-(u32*q(m,acl)/acl)-(u21*r(m,acl)/aco));
den2(m_)=((next^2/(ncl^2))*J*Kp+(σ1*σ2*u21*u32/(aco*acl*nco^2)))*u2*p(m,acl)-
(q(m,acl)*next^2/(nco^2))*Kp+J*r(m,acl)-(s(m,acl)*ncl^2/(u2*nco^2));
Erdoganizq(m_,λcla_,aco_,acl_,nefcla_)=num1(m)/den1(m);
Erdogander(m_,λcla_,aco_,acl_,nefcla_)=num2(m)/den2(m);
(*Modes HE1n (m=1)*)
(*Locate the desired mode visually and find the initial root at the wavelength of 1.7 um*)
h1=Plot({Erdoganizq(1,1.7,a1,acl,nefcla)/I,Erdogander(1,1.7,a1,acl,nefcla)/I,
     {nefcla,1.437,1.43901},PlotRange->{{1.4385,1.43901},{-0.2,0.2}},Frame->True,GridLines->Automatic)
(*Initial value of the effective index*)
nstart=Quiet(FindRoot(Erdoganizq(1,λcla,a1,acl,nefcla1)/I==Erdogander(1,(λcla,a1,acl,nefcla1)/I,
{nefcla1,1.43895},WorkingPrecision->15)((1))((2)));
(*Example: Mode HE11*)
necla={{0,0}};   (*Effectiuve index of the cladding*)
Δneff={{0,0}};(*Effectiuve index difference*)
λcla=1.7;
n11=nstart;
For(i=1,i<=450,i++,
r11cla=FindRoot(Erdoganizq(1,λcla,a1,acl,nefcla1)/I==Erdogander(1,λcla,a1,acl,nefcla1)/I,{nefcla1,n11}))((1))((2));
n11=r11cla;
necla=Append(necla,{λcla,r11cla});
(Δneff=Append(Δneff,{λcla,nefco((i))((2))-n11});
λcla=λcla-0.001;);
necla=Drop(necla,{1});
Δneff=Drop(Δneff,{1});
ListPlot(necla);
ListPlot(Δneff);
```

Table 3. Mathematica code for the calculation of the cladding mode effective index
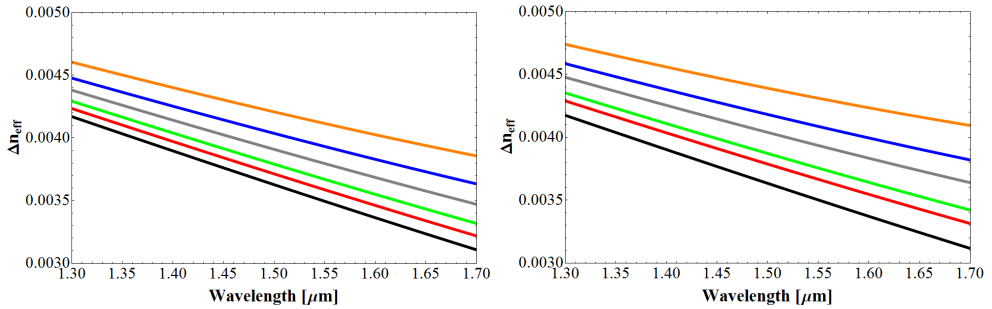
Fig. 6. Effective index difference between the fundamental core mode and HE_{1m} (left graph), and HE_{2m} (right graph) cladding modes.

3.2 Coupled mode equations

In the case of o LPFG, we must consider the coupling between forward propagating modes obeying the coupled mode equations (Bures,2009), which in the case of one forward propagating core mode and forward propagating cladding modes can be written as:

$$\frac{dA_{co}(z)}{dz} = i\sum_{m} B_m(z)C_{co-m}(z) \tag{6a}$$

$$\frac{dB_j(z)}{dz} = iA_{co}(z)C_{j-co} + i\sum_{m\neq j} B_m(z)C_{j-m}(z) \tag{6b}$$

Assuming that the periodic perturbation of the refractive index is much lower that the unperturbed refractive index we can approximate the coupling coefficient by:

$$C_{co-m} = \frac{k}{2\eta_0} \int_{A_\infty} n(r)\delta n(r,z)\,\hat{\mathbf{e}}_{co}^*(r)\cdot\hat{\mathbf{e}}_m(r)e^{-i(\beta_{co}-\beta_m)z}dA \tag{7a}$$

where $C_{m-co}=(C_{co-m})^*$, $\hat{\mathbf{e}}_m(r)$ is the normalized electric field, dA is a differential of area, and the integration is over the infinite area.

Here, we consider the uniform refractive index perturbation δn(r,z) of a three-layered waveguide written as:

$$\delta n(r,z) = \begin{cases} \delta n_{co}e^{i\left(\frac{2\pi}{\Lambda}z+\phi_{co}\right)} & r \leq a_1 \\ \delta n_{cla}e^{i\left(\frac{2\pi}{\Lambda}z+\phi_{cla}\right)} & a_1 \leq r \leq a_2 \\ 0 & r > a_2 \end{cases} \tag{8}$$

Then the coupling coefficient can be written as:

$$C_{co-m} = \frac{k}{2\eta_0} e^{-i\Delta z + i\phi_{co}} \left\{ n_1 \, \delta n_{co} I_{1m} + n_2 \, \delta n_{cla} I_{2m} \right\} \tag{9}$$

where

$$\Delta = \left(\frac{2\pi}{\Lambda} - \frac{2\pi \, \Delta n_{eff}^{co-m}}{\lambda} \right) \tag{10}$$

and

$$I_{1m} = \int_0^{a_1} \hat{\mathbf{e}}_{co}^*(r) \cdot \hat{\mathbf{e}}_m(r) \, r \, dr$$

$$I_{2m} = \int_{a_1}^{a_2} \hat{\mathbf{e}}_{co}^*(r) \cdot \hat{\mathbf{e}}_m(r) \, r \, dr \tag{11}$$

In writing (9) and (10) we have used $\beta_{co} - \beta_m = 2\pi (n_{eco} - n_{ecla}) / \lambda = 2\pi \Delta n_{eff}^{co-m}$, i.e., it is expressed in terms of the effective refractive index difference between the core and cladding modes. The integrals in (11) can be seen as overlapping factors between the core and cladding modes, which determine the changes in the transmission spectrum when there are changes in fibre dimensions, the external refractive index, temperature and stress, since in all cases the effect is to change the effective refractive index of the core and cladding modes.

In order to find an analytical solution for the amplitudes of the core and cladding modes we consider only the coupling to one cladding mode, so that, after differentiating Eqs. (6a) and (6b) and solving the resultant equations we can obtain (Bures, 2009):

$$A_{co}(z) = A_1 \cos\left(\sqrt{\left(\frac{\Delta}{2}\right)^2 + |C_{co-m}|^2} \, z \right) e^{-i\frac{\Delta}{2}z} + B_1 \sin\left(\sqrt{\left(\frac{\Delta}{2}\right)^2 + |C_{co-m}|^2} \, z \right) e^{-i\frac{\Delta}{2}z} \tag{12a}$$

$$B_m(z) = A_2 \cos\left(\sqrt{\left(\frac{\Delta}{2}\right)^2 + |C_{co-m}|^2} \, z \right) e^{i\frac{\Delta}{2}z} + B_2 \sin\left(\sqrt{\left(\frac{\Delta}{2}\right)^2 + |C_{co-m}|^2} \, z \right) e^{i\frac{\Delta}{2}z} \tag{12b}$$

Now we consider specific boundary conditions found in LPFGs, where $A_{co}(0)=1$ and $B_m(z)=0$ which results in (Bures, 2009)

$$A_{co}(z) = \left(\cos\left(\sqrt{\left(\frac{\Delta}{2}\right)^2 + |C_{co-m}|^2} \, z \right) + i \frac{\Delta}{2\sqrt{(\Delta/2)^2 + |C_{co-m}|^2}} \sin\left(\sqrt{\left(\frac{\Delta}{2}\right)^2 + |C_{co-m}|^2} \, z \right) \right) e^{-i\frac{\Delta}{2}z} \tag{13a}$$

$$B_m(z) = i \frac{C_{co-m}}{\sqrt{(\Delta/2)^2 + |C_{co-m}|^2}} \sin\left(\sqrt{\left(\frac{\Delta}{2}\right)^2 + |C_{co-m}|^2} \, z\right) e^{i\frac{\Delta}{2}z - \phi} \qquad (13b)$$

From here we can now write the transmittance at the core as:

$$T_{CO}(z) = \cos^2\left(\sqrt{\left(\frac{\Delta}{2}\right)^2 + |C_{co-m}|^2} \, z\right) + \frac{(\Delta/2)^2}{(\Delta/2)^2 + |C_{co-m}|^2} \sin^2\left(\sqrt{\left(\frac{\Delta}{2}\right)^2 + |C_{co-m}|^2} \, z\right) \qquad (14)$$

This equation is only valid for uniform LPFGs with a step change. For real LPGs, the index change is much more complicated since, for example, in arc induced LPFGs the zone affected by the electric arc spans >300 μm, and is asymmetric in both, the longitudinal and transverse directions. This fact makes the modeling of such gratings a really challenging task. A qualitative analysis of this and other types of gratings can be done only by calculating their effective indices (core and clad) and matching the observed resonance to the calculated dispersion curves of the effective refractive index.

4. Applications of long-period fibre gratings in optical sensing

One of the more important applications of LPFGs is as sensing elements. Owing to the well-known advantages over conventional sensors, such as high resolution, low cost, light weight, and multiplexing possibilities, several optical fibre sensors have evolved from laboratory experiments into commercial products. Although many sensor schemes have been proposed, probably the most popular ones are based on evanescent field interactions (Villatoro et. al. , 2005), fibre Bragg gratings (FBGs) (Othonos & Kalli, 1999), and fibre long period gratings (LPGs) (Vengsarkar et. al., 1996; Vengsarkar & Bhatia, 1996). Fibre gratings have attracted considerable attention as ideal detectors since the information of the physical phenomena is encoded in wavelength. Fibre gratings are very sensitive to physical perturbations like temperature, strain, and pressure (Othonos & Kalli, 1999; Vengsarkar & Bhatia, 1996; Kersey et. al., 1997), however, in combination with a suitable transducer can monitor other magnitudes such as humidity (Liu et. al., 2007), or electric fields (Abramov et. al., 1999). The sensitivity of LPGs to ambient refractive index is higher than that observed in fibre Bragg gratings, mainly due to the fact that in the case of cladding modes the guiding structure is formed by the cladding and the external medium in such way that any change in the ambient refractive index modifies the spectral response of the LPGs (Vengsarkar et. al., 1996; Vengsarkar & Bhatia, 1996).

The potential applications of LPG are strongly determined by the sensitivity of these devices to the influence of the surrounding environment. In general, the performance of devices used in communication, it is expected to have low sensitivity to changes of the surrounding media. By contrast, the LPGs fabricated for sensing applications the characteristics of the devices are designed to enhance its intrinsic sensitivity. Thus, a complete analysis of the sensitivity of LPGs to external ambient is necessary prior to practical devices design. The coupling of the fundamental core mode to cladding modes is determined by the period, the effective refractive index of the core and the cladding. These three parameters, and in consequence the LPG resonant wavelength, will be affected by changes in temperature and strain of the fibre. Additionally, since the cladding modes interact with the buffer or any

other material in close contact with the cladding of the fibre, the wavelength response of the LPG is also affected by the changes in the refractive index of the external medium. Shu et al. (Shu et. al., 2002) have presented a complete investigation of the shift in the center of the wavelength of the resonant peaks of the LPG due to temperature, strain and external refractive index changes, and can be expressed by

$$\Delta\lambda_{res} = \left(\frac{d\lambda_{res}}{dT}\right)\Delta T + \left(\frac{d\lambda_{res}}{dS}\right)\Delta S + \left(\frac{d\lambda_{res}}{dn_{sur}}\right)\Delta n_{sur} \tag{15}$$

where $(d\lambda_{res}/dT)$, $(d\lambda_{res}/dS)$, and $(d\lambda_{res}/dn_{sur})$ are the temperature, strain and surrounding refractive index sensitivity of the resonant wavelength, respectively. In the following sections a detailed expression for such sensitivities is going to present and discussed.

4.1 Temperature sensing with long-period fibre gratings

For more than three decades investigation over optical fibre thermometers has been growing. Early fibre-optic temperature sensors were two fibre interferometers in which temperature was measured by fringe displacements (Hocker, 1979). Later, one-fibre interferometers were proposed and demonstrated that had practically no cross sensitivity (Eickhoff, 1981). Recently, a new generation of fibre-optic temperature sensors based on LPGs has been developed in which temperature is measured in the spectral domain by resonant wavelength shifts, rather than fringe displacements. The vast majority of fibre temperature sensors reported so far have been designed to operate in a range from 20 C to 200 C. However, there are a variety of applications in which high-temperature sensing is important, for example, for monitoring furnace operation or volcanic events, or in fire alarm systems, etc. (Brambilla et. al., 2002). There exist a variety of materials and techniques to fabricate optical fibre thermometers for high temperature. Among them, LPG inscribed with a pulsed CO_2 laser (Davis et. al., 1998), or using an electric arc (Kosinski & Vengsarkar, 1998) have been attracting attention due to their simply fabrication process and their wide range of measurement. The expression for the temperature sensitivity of a LPG, whether is used to measure low- or high-temperature, can be expressed as (Shu et. al., 2002),

$$\frac{d\lambda_{res}}{dT} = \lambda_{res}\left(\alpha_\Lambda + \frac{\alpha_{co}\, n_{co}^{eff} - \alpha_{cl} n_{cl,m}^{eff}}{n_{co}^{eff} - n_{cl,m}^{eff}}\right) \tag{16}$$

where α_Λ is the thermal expansion coefficient of the fibre, α_{co} and α_{cl} are the thermo-optic of core and cladding materials, respectively and γ is the waveguide dispersion described as (Shu et. al., 2002):

$$\gamma = \frac{d\lambda_{res}/d\Lambda}{n_{co}^{eff} - n_{cl,m}^{eff}} \tag{17}$$

In general for silica-based fibre the effect of thermal expansion coefficient is lower than of the thermo-optic, represented by the second term in the parenthesis. However, its influence in the analysis of temperature sensitivity cannot be ignored. For standard fibre, the second term in the parenthesis could be higher than zero, whereas for B–Ge co-doped fibre this

value is lower than zero, because boron doping can decrease significantly the thermo-optic coefficient of the core (Shu et. al., 2001). Thus, it is to be expected that the thermal responses of LPFGs produced in these two fibre types will exhibit opposite trends. It is also evident from eq. (17) that the temperature sensitivity of a LPG is also dependant on the cladding mode excited and in consequence depends on the technique used to fabricate the LPGs.

4.2 Strain sensing with long-period fibre gratings

Grating-based sensors have redefine the concept of "smart structures" since these devices have been successfully integrated or embedded into the materials to allow monitoring of parameters such as load, strain or vibration from which the health of the structure can be evaluated and tracked in a real-time basis. This success is mainly due to the well-known advantages of the optical fibres for sensing, such as EMI immunity, electric passive operation, low weight, small size, and high sensitivity, but also because these grating-based sensors have the inherent self-referencing capability and are easily multiplexed. The strain response of a long-period fibre grating arise due to the physical elongation of the fibre, changing the grating pitch and the effective refractive index of the core and cladding due to the elastooptic effect. The LPG sensitivity to strain can be expressed as follows (Shu et. al., 2002),

$$\frac{d\lambda_{res}}{dS} = \gamma \; \lambda_{res} \left(1 + \frac{\varsigma_{co} \, n_{co}^{eff} - \varsigma_{cl} n_{cl,m}^{eff}}{n_{co}^{eff} - n_{cl,m}^{eff}} \right) \tag{18}$$

where ζ_{co} and ζ_{cl} are the elastooptic coefficient of the core and cladding materials, respectively. The strain response of a LPG depends on the cladding mode excited and the elastooptic coefficient of the core and cladding materials. It can be seen form eq. (18) that a LPG is strain-insensitive when the second term in the parenthesis is equal to -1.

4.3 Refractive index sensing with long-period fibre gratings

The refractive index (RI) is a fundamental material property, in a variety of applications, the measurement of the RI is very important since different chemical substances as well as several physical and biological parameters can be detected through measurements of this parameter. In bio-sensing, for example, there is a need to monitor RI changes on the order of 10^{-4} to 10^{-7} which may be caused by molecular binding, chemical or biochemical reactions, or by changes suffered by a thin bio-layer measure very small RI changes in small volumes of fluid. Traditional bulk refractometers are not appropriate for such an application; in such cases optical fibre refractometers (OFRs) constitute an alternative. OFRs have some advantages over their bulk counterparts, such as high resolution, low cost, light weight, and multiplexing possibilities. Several OFRs based on side-polished single-mode fibre, core-exposed or tapered multimode fibres, fibre Bragg gratings (FBGs), or long period gratings (LPGs) have been reported so far (Lopez-Higuera & Ed., 2002). In a LPG the guided light interacts with the external medium so there is no need to modify the fibre. The effective index of the excited cladding modes depends on the refractive index of the core, cladding and external medium materials. This dependence is clearly observed in the expression derived for the sensitivity of the LPG to external refractive index (Shu et. al., 2002; Miyagi & Nishida, 1979)

$$\frac{d\lambda_{res}}{dn_{ext}} = \gamma\ \lambda_{res}\left(\frac{u_m^2\ \lambda_{res}^3 n_{ext}}{8\pi\, r_{cl}^3\, n_{cl}\left(n_{co}^{eff} - n_{cl,m}^{eff}\right)\left(n_{cl}^2 - n_{ext}^2\right)^{3/2}}\right) \tag{19}$$

u_m is the m-th root of the zeroth-order Bessel function of the first kind, r_{cl} and n_{cl} are the radius and refractive index of the fibre cladding, respectively. In this case is more evident that the sensitivity is rather greater for higher order modes and it can be enhanced by reducing the cladding radius (Martínez-Rios, A. et. al. (2010).) since the term in parenthesis is dependent on (r_{cl}^{-3}).

When the refractive index of the external medium adjacent to the LPG augments the wavelength of the resonant peaks shifts to shorter values. The wavelength changes of the resonant peaks of an arc-induced LPG due to the changes in the external refractive index are shown in graph (a) of the figure 7. The calculated sensitivity of the arc-induced LPG to refractive index changes is 166.66 nm/RIU for a refractive index range of 1.40- 1.46, by contrast in the range of 1-1.39 the sensitivity is only 7.692 nm/RIU. This behavior is also expressed in ec. (4.5), where can be observed that an increment in the external refractive index produce an augment of the sensitivity. In the graph (b) of figure 7 we show the shift of the wavelength resonant peak as the refractive index is changed for an arc-induced LPG that was chemically etched, the final diameter of the cladding was ~39 μm. When the cladding radius decreases, the sensitivity of the of the LPG is highly enhanced as is predicted by the ec. (4.5). The sensitivity of the LPG calculated from the experimental data of graph (b) in Fig. 7 is~3,571 nm/RIU in the range of 1.4-1.46. The sensitivity of an etched-LPG is 1 order of magnitude higher than an unetched LPG. In figure 8 is shown the spectra of an etched arc-induced fibre when the external refractive index changes.
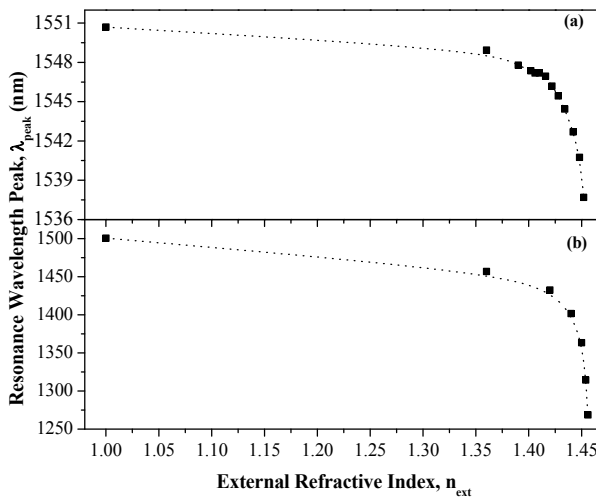

Fig. 7. In these graphs is shown the shift of the resonant wavelength peak when the external refractive index is change. In the upper graph (a) is shown the behavior of an arc-induced LPG when the refractive index of the external medium changes. In the bottom graph (b) the cladding of the LPG fibre was etched, the final diameter was 39 μm.
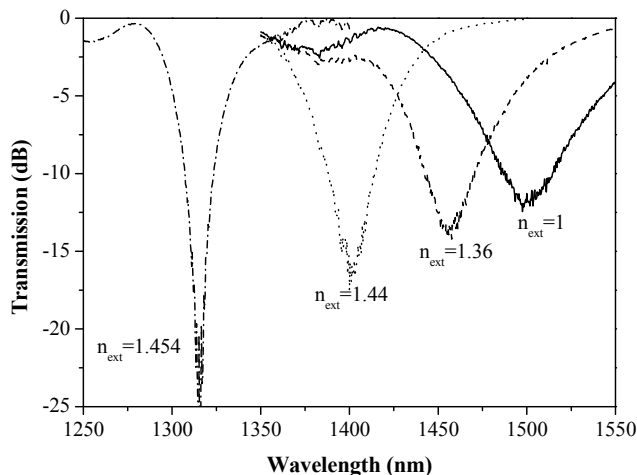
Fig. 8. the spectra transmitted by an arc-induced LPG that was etched to reduce the cladding diameter to 39 μm. As can be seen the resonant peak shifts to shorter wavelengths as the refractive index of the external medium is increased.

5. Conclusion

We have presented a review of the some of the more relevant aspects of LPFGs. Fabrication methods, basic theory and applications have been discussed. As can be clearly seen, LPFGs are sensitive to almost everything, and are used currently in sensor applications and as filters in telecommunication and many other fibre systems. As a sensor their main advantage with respect to fibre Bragg grating based systems is in the lower fabrication cost, since they can be inscribed in almost any type of fibre using a wide variety of forms to change periodically the refractive index in the core, in the cladding, or both. One of the main drawbacks of LPFGs is the bandwidth of notch bands, in the order of 10 nm, which limits the resolution of the measurements. However this can be alleviated by using interferometric arrays consisting of a series of LPFGs which form Mach-Zender interferometers, where the bandwidth may be below 1 nm, similar to fibre Bragg gratings.

6. Acknowledgment

7. References

Abramov, A.; Eggleton, B.; Rogers, J.; Espindola, R.; Hale, A.; Windeler, R. & Strasser, T. (1999). Electrically Tunable Efficient Broad-band Fibre Filter, *IEEE Photonics Technology Letters*, Vol. 11, No. 4, (April 1999), pp. 445-447, ISSN 1041-1135.

Anemogiannis E., Glytsis E. N. & Gaylord T. K.. (2003). Transmission Characteristics of Long-Period Fibre Gratings Having Arbitrary Azimuthal/Radial Refractive Index Variations. *Journal of Lightwave Technology*, Vol. 21, No. 1, (January 2003), pp. 218-227, ISSN 0733-8724.

Arai, T. & Kragic, D. (1999). Variability of Wind and Wind Power, In: *Wind Power,* S.M. Muyeen, (Ed.), 289-321, Scyio, ISBN 978-953-7619-81-7, Vukovar, Croatia

Bilodeau F., Malo B., Albert J., Johnson D. C., Hill K. O., Hibino Y., Abe M. & Kawachi M. (1993). Photosensitization of optical fibre and silica-on-silicon/silica waveguides. *Optics Letters*, Vol. 18, No. 12, (June 1993), pp. 953-955 , ISSN 0146-9592.

Bjarklev. (1986). Microdeformation losses of single-mode fibres with step- index profiles. *Journal of Lightwave Technology*, Vol. 4, No. 3, (March 1986), pp. 341-346, , ISSN 0733-8724.

Brambilla, G.; Kee, H.; Pruneri, V. & Newson, T. (2002). Optical fibre sensors for earth science: From the basic concepts to optimizing glass composition for high temperature applications, *Optics and Lasers in Engineering,* vol. 37, No. 2–3, (February-March 2002), pp. 215–232, ISSN 0143-8166.

Bures J. (2009). Guided Optics:Optical Fibers and All-Fiber Components. WYLEY-VCH (Weinheim, Germany). ISBN 978-3-527-40796-5.

Chan F. Y. & Yasumoto K. (2007). Design of wavelength tunable long-period grating couplers based on asymmetric nonlinear dual-core fibres. *Optics Letters*, Vol. 32, No. 23, (December 2007), pp. 3376-3378, , ISSN 0146-9592.

Chiang K. S.; Liu Y.; Ng M. N.; Dong X. (2000). Analysis of etched long-period fibre grating and its response to external refractive index. *Electonics Letters*, Vol. 36, No. 11, (May 2000), pp. 966-967, ISSN 0013-5194.

Chunn-Yenn L., Wang L. A., Gia-Wei C. (1997). Corrugated long-period fibre gratings as strain, torsion, and bending sensors. *Journal of Lightwave Technology*. Vol. 19, No. 8, (August 2001), pp. 1159-1168, ISSN 0733-8724.

Davis, D.; Gaylord, T.; Glytis, E. & Mettler, S. (1998). CO_2 laser-induced long-period fibre gratings: spectral characteristics, cladding modes and polarization independence, *Electronics Letters,* Vol. 34, No. 14, (July 1998), pp. 1414-1417, ISSN 00-13-5194.

Daxhelet, X. & Kulishov, M. (2003). Theory and practice of long-period gratings: when a loss become a gain. *Optics Letters*, Vol. 28, No. 9,(May 2003), pp. 686-688, ISSN 0146-9592.

DeLisa M. P., Zhang Z., Shiloach M., Pilevar S., Davis C. C., Sirkis J. S. & Bentley W. E. (2000). Evanescent Wave Long-Period Fibre Bragg Grating as an Immobilized Antibody Biosensor. *Analytical Chem*istry, Vol. 72, No. 13, (June 2000), pp. 2895–2900, ISSN 0003-2700.

Dianov E. M., Stardubov D. S., Vasiliev S. A., Frolov A. A., & Medvedkov O. I. (1997). Refractive-index gratings written by near-ultraviolet radiation. *Optics Letters* Vol. 22, No. 4 , (February 1997), pp. 221-223, ISSN 0146-9592.

Eickhoff, W. (1981), Temperature sensing by mode-mode interference in birefringent optical fibres, *Optics Letters*, Vol. *6*, No. 4, (April 1981), pp. 204-206, ISSN 0146-9592.

Erdogan T. (1997). Cladding-mode resonances in short- and long-period fibre grating filters. *Journal of the Optical Society of America A*, Vol. 14, No.8, (August 1997), pp. 1760-2201, ISSN 0740-3232.

Fujimaki M., Ohki Y., Brebner J. L. & Roorda S. (2000). Fabrication of long-period optical fibre gratings by use of ion implantation. *Optics Letters*. Vol. 25, No. 2, (January 2000), pp. 88-89, ISSN 0146-9592.

Gu Z., Xu Y. & Gao K. (2006).Optical fibre long-period grating with solgel coating for gas sensor. *Optics Letters*, Vol. 31, No. 16, (August 2006), pp. 2405-2407, ISSN 0146-9592.

Hill K. O., Malo B., Vineberg K. A., Bilodeau F., Johnson D. C.& Skinner I. (1990). Efficient mode conversion in telecommunication fibre using externally written gratings. *Electronics Letters*, Vol. 26, No 16, (August 1990), pp. 1270-1272, ISSN 0013-5194.

Hocker, G. (1979). Fibre-optic sensing of pressure and temperature, *Applied Optics,* Vol. 18, No.9, (May 1979), pp. 1445-1448, ISSN 003-6935.

Hwang I. K., Yun S. H. & Kim B. Y.. (1999). Long-period fibre gratings based on periodic microbends. *Optics Letters,* Vol. 24, No. 18, (September 1999), pp. 1263-1265, ISSN 0146-9592.

J. Lopez-Higuera, J. Ed., (2002). *Handbook of Optical Fibre Sensing Technology*, ISBN 978-0-471-82053-6 Wiley, New York, USA

Jeong Y., Yang B., Lee B., Seo H. S., Choi S., Oh K. (2000). Electrically controllable long-period liquid crystal fibre gratings. *Photonics Technology Letters*, Vol. 12, No. 519-521, (May 2000), pp. 519 – 521, ISSN 1041-1135.

Kersey, A.; Davis, M.; Patrick, H.; LeBlanc, M.; Koo, K.; Askins, C.; Putnam, M. & Friebele, E. (1997). Fibre Grating Sensors, *Jorunal of Lightwave Technology,* Vol. 15, No. 8, pp. 1442-1462, ISSN 0733-8724.

Kosinski, S., & Vengsarkar, A. (1998). Splicer-based long-period fiber gratings, *Optical Fibre Communication Conference*, Vol. 2 of 1998 OSA Technical Digest Series (Optical Society of America, 1998), ISBN 1557525293, paper ThG3..

Lemaire P. J., Atkins R. M., Mizrahi V. & Reed W. A. (1993). High pressure H_2 loading as a technique for achieving ultrahigh UV photosensitivity and thermal sensitivity in GeO_2 doped optical fibres, *Electronics Letters*, Vol. 29, No. 13, (June 1993), pp. 1191-1193, ISSN 0013-5194.

Li, B.; Xu, Y. & Choi, J. (1996). Applying Machine Learning Techniques, *Proceedings of ASME 2010 4th International Conference on Energy Sustainability*, pp. 14-17, ISBN 842-6508-23-3, Phoenix, Arizona, USA, May 17-22, 2010

Lima, P.; Bonarini, A. & Mataric, M. (2004). *Application of Machine Learning,* InTech, ISBN 978-953-7619-34-3, Vienna, Austria

Liu, Y.; Wang, L.; Zhang, M.; Tu, D.; Mao, X. & Lia, L (2007). Long-Period Grating Relative Humidity Sensor with Hydrogel Coating, *IEEE Photonics Technology Letters*, Vol. 19, No. 12,(June 2007), pp.880-882, ISSN 1041-1135.

Martínez-Rios, A.; Monzón-Hernández, D., & Torres-Gomez, I, (2010). Highly sensitive cladding-etched arc-induced long-period fibre gratings for refractive index sensing, *Optics Communications*, Vol. 283, No. 6, (March 2010), pp. 958-962, ISSN 0030-4018.

Miyagi, M. & Nishida, S., (1979). An approximate formula for describing dispersion properties of optical dielectric slab and fibre waveguides, Journal of the Optical Society of America Vol 69, No.2, (February 1997), pp. 291-293, ISSN 0030-3941.

Mohamed W. & Gu X. (2009). Long-period grating and its application in laser beam shaping in the 1.0 μm wavelength region, *Applied Opt*ics. Vol. 48, No. 12, (April 2009), pp. 2249-2254, ISSN 003-6935.

Ng M. N. & Chiang K. S. (2002). Thermal effects on the transmission spectra of long-period fibre gratings. *Optics Communications*, Vol. 208, No. 4-6, (July 2002), pp. 321-327, ISSN 0030-4018.

Othonos, A & Kalli, K. (1999). *Fibre Bragg Gratings: Fundamentals and Applications in Telecommunications and sensing,* Artech House, ISBN 0-89006-344-3, Norwood, MA, USA

Rao Y.J., Zhu T., Ran Z. L., Wang Y. P., Jiang J. & Hu A. Z. (2004). Novel long-period fibre gratings written by high-frequency CO2 laser pulses and applications in optical fibre communication. *Optics Communications*, Vol. 229, No. 1-6, (January 2004), pp. 209–221, ISSN 0030-4018.

Savin S., Digonnet M. J. F., Kino G. S & H. J. (2000). Tunable mechanically induced long-period fibre gratings. *Optics Letters*, Vol. 25, No. 10, (May 2000), pp. 710 – 712, ISSN 0146-9592.

Shu Y., Lu C., Lacquet B. M., Swart P. L. & Spammer S. J. (2002). Wavelength-tunable add/drop multiplexer for dense wavelength division multiplexing using long-period gratings and fibre stretchers. Optics Communications, Vol. 208, No. 4-6, (July 2002), pp. 337-344, ISSN 0030-4018.

Shu, X.; Allsop, T.; Zhang, L. & Bennion, (2001). High-Temperature Sensitivity of Long-Period Gratings in B–Ge Codoped Fibre, *IEEE Photonics Technology Letters*, Vol. 13, No. 8, (August 2001), pp. 818-820, ISSN 1041-1135.

Shu, X.; Zhang, L. & Bennion, I. (2002). Sensitivity Characteristics of Long-Period Fibre Grating, *Journal of Ligthwave Technology*, Vol. 20, No.2, pp.255-266, ISSN 0733-8724.

Siegwart, R. (2001). Indirect Manipulation of a Sphere on a Flat Disk Using Force Information. *International Journal of Advanced Robotic Systems,* Vol.6, No.4, (December 2009), pp. 12-16, ISSN 1729-8806

Su C. D. & Wang L. A. (1999). Effect of Adding a Long Period Grating In a Double-Pass Backward Er-Doped Superfluorescent Fibre Source. *Journal of Lightwave Technology.* Vol. 17, No. 10, (October 1999), pp. 1896-1903, ISSN 0733-8724.

Van der Linden, S. (June 2010). Integrating Wind Turbine Generators (WTG's) with Energy Storage, In: *Wind Power,* 17.06.2010.

Vaziri M. & Chin-Lin C.. (1997). An etched two-mode fibre modal coupling element. *Journal of Lightwave Technology.* Vol. 15, No. 3, (March 1997), pp. 474-481, ISSN 0733-8724.

Vengsarkar A.N., Lemaire P. J., Judkins J. B., No. Bhatia B., Erdogan T & Sipe J. E. (1996). Long-period fibre gratings as band-rejection filters, *Journal of Lightwave Technology*, Vol. 14, No. 1 , (January 1996), pp. 58-65, ISSN 0733-8724.

Vengsarkar, A. & Bhatia, B. (1996). Optical Fibre Long-Period Fibre Sensors, *Optics Letters*, Vol. 21, No. 9, (May 1996), pp. 692-694, ISSN 0146-9592.

Vengsarkar, A.; Lemaire, P.; Judskin J.; Bhatia, B.; Erdogan, T. & Sipe, J. (1996). Long-Period Fibre Gratings as Band-Rejection Filters, *Journal of Lightwave Technology*, Vol. 14, No. 1, (January 1996) pp. 58-64, ISSN 0733-8724.

Villatoro, J.; Monzón-Hernández, D. & Mejía, E. (200). Fabrication and modeling of uniform-waist single-mode tapered optical fibre sensors, *Applied Optics*, Vol. 42, No. 13, (May 2003), pp. 2278-2283, ISSN 0003-6935.

Williams D. L., Ainslie B. J., Armitage J. R., Kashyap R., Campbell R. (1993). Enhanced UV photosensitivity in boron codoped germanosilicate fibres. *Electronics Letters*, Vol. 29, No. 1, (January 1993), pp. 45-47, ISSN 0013-5194.

Zhang L., Liu Y., Everall L., Williams J. A. R. & Bennion I. (1999). Design and realization of long period grating devices in conventional and high birefringence fibre and their novel applications as fibre-optic load sensor. *IEEE Journal of Selected Topics in Quantum Electronics*, Vol. 5, No. 5, (September/October 1999), pp. 1373-1378, ISSN 1077-260X.

Fiber Optic Sensors

Edited by Dr Moh. Yasin

This book presents a comprehensive account of recent advances and researches in fiber optic sensor technology. It consists of 21 chapters encompassing the recent progress in the subject, basic principles of various sensor types, their applications in structural health monitoring and the measurement of various physical, chemical and biological parameters. It also highlights the development of fiber optic sensors, their applications by providing various new methods for sensing and systems, and describing recent developments in fiber Bragg grating, tapered optical fiber, polymer optical fiber, long period fiber grating, reflectometry and interefometry based sensors. Edited by three scientists with a wide knowledge of the field and the community, the book brings together leading academics and practitioners in a comprehensive and incisive treatment of the subject. This is an essential reference for researchers working and teaching in optical fiber sensor technology, and for industrial users who need to be aware of current developments and new areas in optical fiber sensor devices.

How to reference

In order to correctly reference this scholarly work, feel free to copy and paste the following:

Alejandro Martinez-Rios, David Monzon-Hernandez, Ismael Torres-Gomez and Guillermo Salceda-Delgado (2012). Long Period Fibre Gratings, Fiber Optic Sensors, Dr Moh. Yasin (Ed.), ISBN: 978-953-307-922-6, InTech, Available from: http://www.intechopen.com/books/fiber-optic-sensors/long-period-fibre-gratings

INTECH
open science | open minds